31st Congress of the International Council of the Aeronautical Sciences

Belo Horizonte, Brazil; September 09-14, 2018

BI-LEVEL TRAJECTORY OPTIMIZATION BY STOCHASTIC COLLOCATION FOR UNCERTAINTY INTERVAL CALCULATION

Patrick Piprek* **and Florian Holzapfel***

* **Technical University of Munich, Institute of Flight System Dynamics, Bolzmannstrasse 15, 85748 Garching bei Muenchen, Germany**

Keywords: *generalized polynomial chaos, direct optimal control, uncertain trajectory optimization, bi-level optimal control, worst-case quantification*

Abstract

This study presents a bi-level framework designed for the optimal control (OC) of aircraft. Overall, the goal is to calculate trajectories for the aircraft under external and internal uncertainties that give a worst-case approximation of the uncertainty interval.
The bi-level OC framework is set up as follows: Within the lower level, standard deterministic trajectory optimization problems by gradient-based optimization are solved. The solved problems only differ in their numerical values set for the uncertain parameters. It should be noted that this makes it easy to parallelize them, as they are independent of each other. The calculation of the uncertain response of the system is based on the generalized polynomial chaos (gPC) method. The upper level problem provides the numerical values of the uncertain parameters and is optimized using a differential evolution (DE) strategy. Thus, the connection from the upper to the lower level are the numerical values of the uncertain parameters. Conversely, the lower level provides the upper level with the optimized trajectory at each of the uncertain parameter's positions yielding the statistical moments.
We use case studies from a vertical take-off and landing vehicle (VTOL) transition maneuvers to show the viability of the approach.

1 Introduction

The use of gPC [1] is very popular within the engineering research community to model the effects of uncertainties in dynamic systems. It is for instance used within heat transfer problems [2], flow simulations [3], and spacecraft attitude propagation [4]. Normally, the upcoming expansion integrals are solved using the stochastic collocation (SC) approach by applying a Gaussian quadrature [5]. Within this study, we use the SC approach with LAGRANGE polynomials instead of the standard Gaussian quadrature [5].
That is done due to the following reason: With the Gaussian quadrature approach, there are predefined expansion nodes where the system must be evaluated. This is very simple to program but lacks the quality to quantify the error of the expansion. This is generally also not possible with the LAGRANGE polynomials in the standard setup for the SC [5]: But, with the proposed bi-level OC formulation we are able to provide an idea of the approximation error and in some sense the worst-case result.
This quantification of the accuracy of the gPC expansion recently became a more researched topic within the community [6, 7, 8, 9]: Study [6] uses Monte-Carlo (MC) techniques to verify the results of gPC. The authors as well compare gPC expansions to analytic solutions obtained for simplified problems and showed their accordance.

However, this method still relies on a sampling based MC techniques, where convergence speed is slow and unknown a priori.
The authors of study [7] again use MC methods to verify their gPC method that is based on Stieltjes procedure for the construction of orthogonal polynomials. The authors apply the method to crosstalk simulation and receive a good approximation quality.
Again, the MC method is used in [8] to quantify uncertainties within a stochastic system. Additionally, the authors introduce accuracy, convergence (in approximation and moment), and error analysis methods. Here, they especially consider the accuracy of the statistical moments calculation.
Finally, study [9] compares the gPC expansion to different Kalman filter implementations for uncertainty quantification. Furthermore, the authors compare their results with a MC method to verify them.
From the previous literature research it is evident that most of the methods used to verify gPC expansions are based on MC methods. This study, on the other hand, introduces a new method for gPC verification based on a bi-level OC scheme. This framework should enhance the approximation capabilities and provide results on a global scale.
The study is organized as follows: Section 2 introduces the gPC method in general and the LAGRANGE interpolation SC method in specific. Additionally, it introduces the calculation of the statistical moments. Within section 3, the proposed bi-level OC setup is explained. Therefore, both the lower level, gradient-based OC problem formulation is introduced as well as the combination of gPC and lower level to the bi-level framework. The test case, including the optimization model, is introduced in section 4, while conclusive remarks are given in section 5.

2 Generalized Polynomial Chaos

The gPC expansion was developed by XIU and KARNIADAKIS in [1] and is an extension of NORBERT WIENER'S work on Gaussian uncertainties [10]. Within subsection 2.1 the definition of gPC is stated, while subsection 2.2 introduces the LAGRANGE interpolation approach to calculate the gPC expansion. Subsection 2.3 gives some remarks on the computation of the statistical moments by using the gPC expansion with LAGRANGE polynomials.

Table 1: Continuous probability distribution - orthogonal polynomial connection within Wiener-Askey scheme (after [5])

Probability Distribution	Support Ω	Orthogonal Polynomial
Gaussian/Normal	$]-\infty,\infty[$	Hermite
Gamma	$[0,\infty[$	Laguerre
Beta	$]-1,1[$	Jacobi
Uniform	$]-1,1[$	Legendre

2.1 Definition

The gPC expansion is defined by a Fourier-like expansion formula as follows [5]:

$$\mathbf{y}(\mathbf{z};\theta) \approx \sum_{m=0}^{M-1} \hat{\mathbf{y}}_m(\mathbf{z})\,\Phi_m(\theta) \tag{1}$$

Thus, gPC decomposes the uncertain system response $\mathbf{y} \in \mathbb{R}^{n_y \times 1}$ into a finite sum approximation of order M. Here, the expansion consists of expansion coefficients $\hat{\mathbf{y}} \in \mathbb{R}^{n_y \times M}$ that only depend on the deterministic parameters $\mathbf{z} \in \mathbb{R}^{n_z \times 1}$, while the uncertain parameters $\theta \in \mathbb{R}^{n_\theta \times 1}$ are only related to the orthogonal polynomials $\Phi \in \mathbb{R}^{M \times 1}$.
The appropriate orthogonal polynomial basis is given by the WIENER-ASKEY SCHEME and is only dependent of the probability distribution of the uncertain parameters. This is depicted in Table 1 for some continuous distributions in gPC.
Generally, the only remaining issue in solving Eq. 1 is the determination of the expansion coefficients. This is achieved by a LAGRANGE interpolation within this study that approximates the coefficients as a whole (subsection 2.2).

2.2 Lagrange Interpolation

One of the simplest approximations of Eq. 1, i.e., the complete polynomial chaos, is given by a LA-

GRANGE interpolation as follows:

$$\begin{aligned}\mathbf{y}(\mathbf{z};\theta) &\approx \sum_{m=0}^{M-1} \hat{\mathbf{y}}_m(\mathbf{z})\,\Phi_m(\theta) \\ &\approx \sum_{m=0}^{M-1} \tilde{\mathbf{y}}_m(\mathbf{z})\,\mathscr{L}_m(\theta)\end{aligned} \tag{2}$$

This basically removes the task to calculate the expansion coefficients of Eq. 1 by e.g., SC [5] due to the fact that the gPC expansion is approximated as a whole by the LAGRANGE coefficients $\tilde{\mathbf{y}} \in \mathbb{R}^{n_y \times M}$. These coefficients are calculated as sample solutions at nodes specified by the user. The chosen nodes must represent the system response surface accurately. The nodes are then also part of the LAGRANGE interpolation polynomial (Eq. 3).
The LAGRANGE interpolation polynomial itself is defined as follows [11]:

$$\mathscr{L}_j(\theta) = \prod_{\substack{i=1 \\ i\neq j}}^{n} \frac{\theta - \theta_i}{\theta_j - \theta_i} \tag{3}$$

Take into account that this gives an approximation of the gPC for all possible probability distributions and not only the ones within the WIENER-ASKEY SCHEME that have a corresponding orthogonal polynomial (Table 1).
A disadvantage of the method is that the calculation of statistical moments is more sophisticated than for the normal SC approach [5] and the selection of the evaluation nodes for the LAGRANGE polynomials in Eq. 3 is not straightforward. Especially, the selection of evaluation nodes is addressed within this study as we use the upper level of the bi-level OC formulation for this task.

2.3 Statistical Moments

Statistical moments are straightforward to write down for the gPC expansion using LAGRANGE interpolation, but require the numerical evaluation of an integral for the LAGRANGE polynomial over the uncertainty domain. This is generally very time consuming, but can be handled as a pre-processing step using symbolic derivations.

For instance, the mean $\mathbb{E}$ is calculated as follows:

$$\mathbb{E}[\mathbf{y}(\mathbf{z};\theta)] \approx \sum_{m=0}^{M-1} \tilde{\mathbf{y}}_m(\mathbf{z}) \int_{\Omega} \mathscr{L}_m(\theta)\,\rho(\theta)\,\mathrm{d}\theta \tag{4}$$

The calculation of higher order moments is straightforward and can be achieved using the standard definition for e.g., variance or skewness [11]. Consequently, this requires the integration of higher order products of LAGRANGE polynomials.

3 Bi-level Framework

This section introduces the proposed bi-level OC methodology used to calculate the worst-case approximations of the uncertainty interval for the trajectories. Subsection 3.1 introduces the general OC problem, while subsection 3.2 gives an overview of the proposed bi-level framework.

3.1 Trajectory Optimization Problem

The trajectory optimization problem is formulated as follows [12]:

$$\begin{aligned}\min_{\mathbf{z},t_f} \quad & J = e(\mathbf{z}) + \int_{t_0=0}^{t_f} L(\mathbf{z})\,\mathrm{d}t \\ \text{s.t.} \quad & \mathbf{f}(\mathbf{z};\theta) = \dot{\mathbf{x}}, \\ & \mathbf{c}(\mathbf{z}) \leq \mathbf{0}, \\ & \boldsymbol{\psi}(\mathbf{z}) = \mathbf{0}\end{aligned} \tag{5}$$

Within the formulation of Eq. 5, the OC goal is to minimize the cost functional J that is split up into a final value term e (Mayer term) and an integrated term L (Lagrange term). The minimization is subject to equality $\mathbf{c} \in \mathbb{R}^{n_c \times 1}$ and inequality $\boldsymbol{\psi} \in \mathbb{R}^{n_\psi \times 1}$ path and point constraints respectively. A specialty of OC is that one equality path constraint is reserved for the state dynamics $\dot{\mathbf{x}} \in \mathbb{R}^{n_x \times 1}$ that depend on the states $\mathbf{x} \in \mathbb{R}^{n_x \times 1}$ and controls $\mathbf{u} \in \mathbb{R}^{n_u \times 1}$. These are combined in the previously introduced parameter vector $\mathbf{z}$. In our case the state dynamics also depend on the uncertain parameters.
The OC problem is transcribed using direct methods [12] by the OC toolbox `FALCON.m` [13] and solved using the solver `Ipopt` [14].

3.2 Combination of Generalized Polynomial Chaos and Trajectory Optimization in Bi-level Framework

Within our approach to calculate worst-case approximations of trajectories with uncertainties, we rely on a bi-level methodology. The structure of the proposed bi-level framework is illustrated in Figure 1: Within the lower level multiple trajectory optimization problems are solved by using gradient-based optimization (subsection 3.1). The upper level solves a parameter optimization problem by using a DE strategy [15]. This strategy assures a global optimal solution.
The lower level cost functions are standard for trajectory optimization, i.e., minimal time or minimal fuel consumption. Conversely, the upper level tries to e.g., maximize the variance of the solution to find a worst-case bound.
Both levels are connected by parameter exchange: The upper level supplies the lower level with evaluation parameters for the uncertainties, i.e., the evaluation points of the LAGRANGE polynomials. Then, the lower level provides the upper level with the optimal trajectories at these nodes that are used for the statistical moment calculation. Overall, the framework tries to balance the aim of the upper level to optimize its cost and the aim of the lower levels to optimize their costs individually. By this, worst-case scenarios that are still achievable by the aircraft can be calculated.
The proposed bi-level structure offers the three following advantages: First of all, the general problem of the SC with LAGRANGE polynomials for the standard gPC application, i.e. the choice of accurate nodes in order to reproduce the uncertain response with suitable accuracy, is overcome. This is based on the fact that the upper level finds suitable nodes for the optimization of its cost function, while it also fulfills the lower level trajectory optimization problem.
Another issue, related to gPC by discrete expansion [5], can also be overcome by the framework: The accuracy of the moments is unknown for the discrete expansion approach, because it is depending on the order of the expansion and also the nonlinearity of the uncertain response surface. Now, the proposed approach overcomes this issue with a suitable upper level cost functional, e.g., the maximization of the variance, such that worst-case approximations can be found.
Finally, the usage of LAGRANGE polynomials offers another advantage concerning the discrete expansion: With the LAGRANGE polynomial approach it is no longer necessary that an orthogonal polynomial basis exists. Therefore, we can also simply model uncertainties that have no corresponding orthogonal polynomial in the WIENER-ASKEY SCHEME (Table 1; e.g., the Weibull distribution).
Overall, the proposed bi-level framework is a cooperative bi-level approach, because both the upper and the lower level work together to optimize the overall cost functional of both levels and try to achieve a worst-case approximation. This is e.g., the case for a variance maximization, i.e., the calculation of a worst-case variance, presented in section 4.

4 Case Studies

This section introduces the case studies and results for the proposed bi-level methodology of this study (section 3). Here, subsection 4.1 introduces the optimization model, while the optimization results are given in subsection 4.2.

4.1 Optimization Model

The optimization model is based on a rigid-body representation of a VTOL on a fixed-flat earth [16]. The twelve states comprise the position (x, y, z), the velocity (u, v, w), the orientation (ϕ, θ, ψ), and the rotation (p, q, r). The VTOL and the aforementioned definitions are also illustrated in Figure 2.
As controls, the rotor speeds ω_1 (left wing), ω_2 (right wing), ω_3 (front fuselage), and ω_4 (rear fuselage) are used. Additionally, the deflection of the elevator η and the tilt of the first and second rotor δ_1 and δ_2 are available.

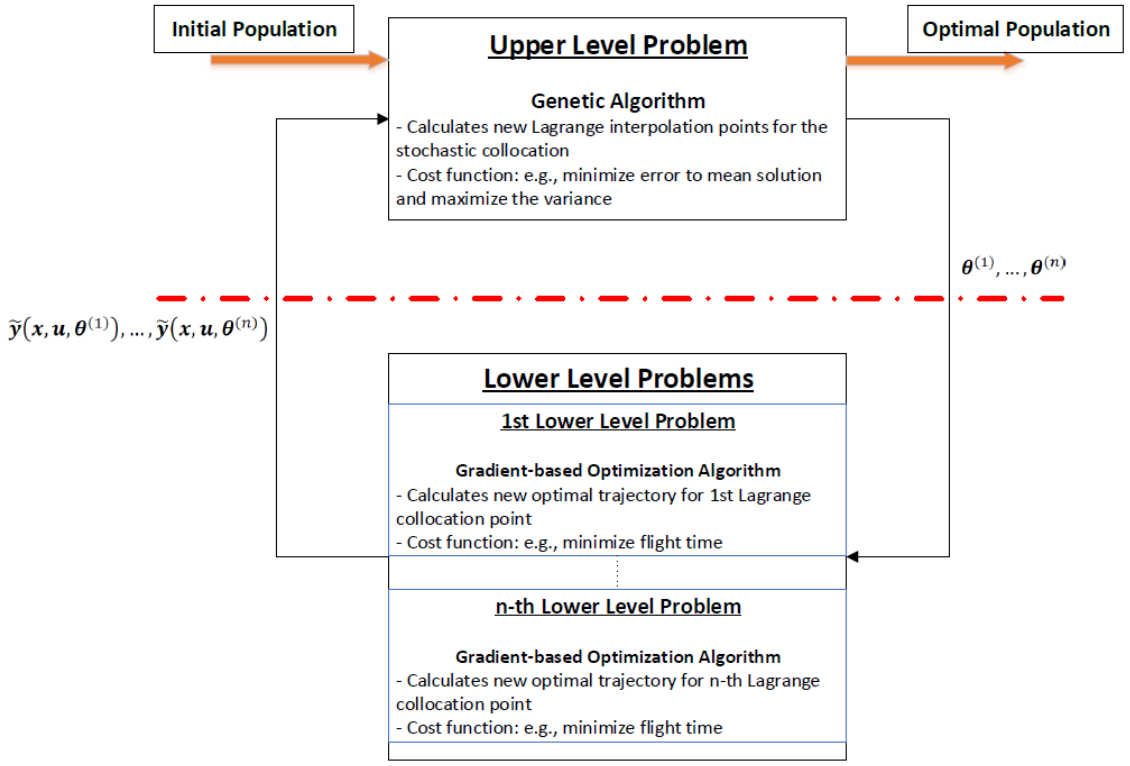

Fig. 1 : Structure of the bi-level framework for worst-case uncertainty interval calculation.

Now, the rigid-body equations of motion are given as follows [16]:

$$\begin{aligned}\dot{\mathbf{x}} &= \left[\dot{x}, \dot{y}, \dot{z}, \dot{u}, \dot{v}, \dot{w}, \dot{\phi}, \dot{\theta}, \dot{\psi}, \dot{p}, \dot{q}, \dot{r}\right]^T \\ &= \begin{bmatrix} \mathbf{0}_3 & \mathbf{P} & \mathbf{0}_3 & \mathbf{0}_3 \\ \mathbf{0}_3 & -\Omega & \mathbf{0}_3 & \mathbf{0}_3 \\ \mathbf{0}_3 & \mathbf{0}_3 & \mathbf{0}_3 & \mathbf{O} \\ \mathbf{0}_3 & \mathbf{0}_3 & \mathbf{0}_3 & -\mathbf{I}^{-1}\Omega\mathbf{I} \end{bmatrix} \mathbf{x} \\ &+ \begin{bmatrix} \mathbf{0}_{3\times 1} \\ \frac{\mathbf{F}}{m} \\ \mathbf{0}_{3\times 1} \\ \mathbf{I}^{-1}\mathbf{M} \end{bmatrix}\end{aligned} \tag{6}$$

The zero matrices of appropriate size, denoted by their index, are given by $\mathbf{0}$ in Eq. 6 (a single index indicates a square matrix). The inertia tensor is $\mathbf{I}$, the mass m, while the forces and moments, consisting of aerodynamics, thrust, and gravitation, are summarized in the terms $\mathbf{F}$ and $\mathbf{M}$ respectively. The matrix Ω is the skew-symmetric matrix for the cross product and contains the rotation states. The matrix $\mathbf{P}$ and $\mathbf{O}$ are the position and attitude propagation matrices respectively and defined as follows [16]:

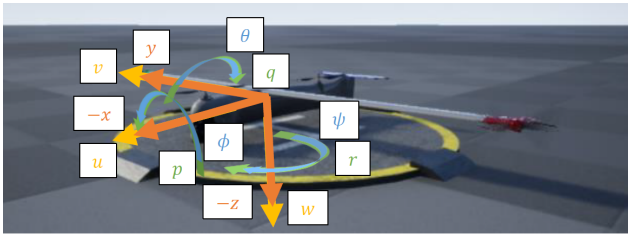

Fig. 2 : Side view of VTOL including linear and rotational axes definition with the corresponding states with exchange between both levels.

$$\mathbf{P} = \begin{bmatrix} -1 & 0 & 0 \\ 0 & 1 & 0 \\ 0 & 0 & -1 \end{bmatrix} \tag{7}$$

$$\mathbf{O} = \begin{bmatrix} 1 & \tan(\theta)\sin(\phi) & \tan(\theta)\cos(\phi) \\ 0 & \cos(\phi) & \sin(\phi) \\ 0 & \frac{\sin(\phi)}{\cos(\theta)} & \frac{\cos(\phi)}{\cos(\theta)} \end{bmatrix} \tag{8}$$

For the optimization case in subsection 4.2, the states, controls, and outputs are bounded, scaled, and offset as defined in Table 2.
The VTOL flies a transition maneuver from hover

Table 2: States, controls, and outputs bounds, scaling, and offset for optimization.

Symbol	Lower Bound	Upper Bound	Scaling	Offset
States				
x	$-\infty$	$+\infty$	1	$0m$
y	$-\infty$	$+\infty$	1	$0m$
z	$0m$	$+25m$	1	$0m$
ϕ	$-45°$	$+45°$	1	$0°$
θ	$-75°$	$+75°$	1	$0°$
ψ	$-\infty$	$+\infty$	1	$0°$
u	$+10^{-7}\frac{m}{s}$	$+50\frac{m}{s}$	1	$0\frac{m}{s}$
v	$-10\frac{m}{s}$	$+10\frac{m}{s}$	1	$0\frac{m}{s}$
w	$-10\frac{m}{s}$	$+10\frac{m}{s}$	1	$0\frac{m}{s}$
p	$-30\frac{°}{s}$	$+30\frac{°}{s}$	1	$0\frac{°}{s}$
q	$-30\frac{°}{s}$	$+30\frac{°}{s}$	1	$0\frac{°}{s}$
r	$-15\frac{°}{s}$	$+15\frac{°}{s}$	1	$0\frac{°}{s}$
Controls				
ω_1	$+0\frac{rad}{s}$	$+1570.8\frac{rad}{s}$	1	$+750\frac{rad}{s}$
ω_2	$+0\frac{rad}{s}$	$+1570.8\frac{rad}{s}$	1	$+750\frac{rad}{s}$
ω_3	$+0\frac{rad}{s}$	$+1570.8\frac{rad}{s}$	1	$+750\frac{rad}{s}$
ω_4	$+0\frac{rad}{s}$	$+1570.8\frac{rad}{s}$	1	$+750\frac{rad}{s}$
η	$-25°$	$+25°$	1	$0°$
δ_1	$-30°$	$+120°$	1	$+43°$
δ_2	$-30°$	$+120°$	1	$+43°$
Outputs				
Kinematic Velocity V_K	$+10^{-7}\frac{m}{s}$	$+25\frac{m}{s}$	1	$+10\frac{m}{s}$
Funnel Distance d_F	$+0.1m$	$+\infty$	1	$0m$

to fixed-wing mode with the initial and final boundary conditions defined in Table 3. While transitioning, it also escapes from a funnel. The distance to the funnel is hereby defined as follows:

$$d_F = z - s(x,y) \tag{9}$$

In Eq. 9, the function $s(x,y)$ is a sigmoid that models the escape funnel and is defined as follows:

$$s(x,y) = s_{scale} \cdot \frac{\exp\left(\sqrt{x^2+y^2}+s_{off}\right)}{\exp\left(\sqrt{x^2+y^2}+s_{off}\right)+1} + s_{shift} \tag{10}$$

The sigmoid design parameters are chosen as follows: $s_{scale} = 5$, $s_{off} = -2$, and $s_{shift} = -1$. These denote the scaling, offset, and shift parameter of the sigmoid function $s(x,y)$ respectively.

4.2 Optimization Results

The lower level optimizations are calculated with respect to the following cost function:

$$J = t_f \tag{11}$$

Thus, we are optimizing the problem to achieve a minimal transition time.

Table 3: Initial and final state and output conditions for the optimization.

Symbol	Initial Value Bounds	Final Value Bounds
States		
x	$0m$	free
y	$0m$	free
z	$+0.1m$	$\geq +4.5m$
ϕ	$0°$	$0°$
θ	$0°$	free
ψ	$0°$	$0°$
u	$+0.1\frac{m}{s}$	free
v	$0\frac{m}{s}$	$0\frac{m}{s}$
w	$0\frac{m}{s}$	free
p	$0\frac{°}{s}$	$0\frac{°}{s}$
q	$0\frac{°}{s}$	$0\frac{°}{s}$
r	$0\frac{°}{s}$	$0\frac{°}{s}$
Outputs		
V_K	auto set	$\geq +20\frac{m}{s}$
γ_K	free	$[-0.5;+0.5]°$

In the following we look at two case studies in order to test the bi-level framework proposed in subsection 3.2: At first, subsection 4.2.1 looks at the maximization of the final time variance. Then, subsection 4.2.2 gives further results related to the maximization of the position standard deviation. Both test cases also minimize the distance to their respective mean values to assure a comparability with the standard gPC results. Additionally, the results for different gPC orders ranging from $M = 2-5$ are looked at.
It should be noted that the reference (comparison) results are calculated using the gPC expansion by Gaussian quadrature as introduced in [5].
Take into account that the sidewards wind velocity has been chosen as the uncertainty with a UNIFORM distribution defined as follows:

$$v_W \in U\left(-5\frac{m}{s}, +5\frac{m}{s}\right) \tag{12}$$

4.2.1 *Maximization of Final Time Variance*

This section summarizes the test case results for the case study with maximization of the final time variance using the proposed bi-level framework. As mentioned before a minimization to the reference mean final time is also sought to make the results comparable.
Table 4 summarizes the results for the bi-level

Table 4: Results for the maximization of the final time variance for different expansion order.

Order	$\mathbb{E}\left[t_f\right]$ (gPC)	$\mathbb{E}\left[t_f\right]$ (BL)	$\sigma\left[t_f\right]$ (gPC)	$\sigma\left[t_f\right]$ (BL)
2	$1.4003s$	$1.3905s$	$0.00020838s$	$0.00088112s$
3	$1.3925s$	$1.3821s$	$0.00043615s$	$0.0036978s$
4	$1.3881s$	$1.3767s$	$0.0010594s$	$0.0016458s$
5	$1.3921s$	$1.3823s$	$0.0010851s$	$0.020941s$

(BL) and the standard gPC optimization (gPC) for different orders. Additionally, Table 5 summarizes the results for the optimized node positions of the LAGRANGE polynomials.

Now the results are described: First of all, Table 4 shows that the mean value matching is achieved fairly well and that therefore it is reasonable to compare the results. Additionally, it can be observed that the expansion of order 2 depicts the problems related to low order gPC expansion that these cannot accurately cover higher order moments (in this case the standard deviation). In this example the problem is overcome with the 4^{th} and 5^{th} order expansion that seem to converge to a standard deviation and a mean value ($\mathbb{E}\left[t_f\right] \approx 1.39s$ and $\sigma\left[t_f\right] \approx 0.001s$).

Now the bi-level framework shows that the 3^{rd} and 5^{th} order expansion create the highest standard deviations. This behavior is also seen in Table 5: Here, the 3^{rd} and 5^{th} order expansion shift their nodes both towards negative velocities. This seems to be the shift direction to a worst-case approximation of the standard deviation. It can further be observed from the results that polynomials with an odd highest order exponent seem to approximate the response in a better way and therefore lead to the possibility of a worst-case approximation. Following this argumentation it is reasonable to assume that also the real system response surface is related to a polynomial with odd highest order exponent.

Overall, the results of this subsection depict that the proposed bi-level framework is able to approximate a worst-case statistical moment response of an uncertain system. Now, subsection 4.2.2 continues with a more sophisticated example.

Table 5: Node positions for the bi-level results to optimize the final time variance with different expansion order.

Order	2	3	4	5
Nodes	$\begin{bmatrix} -1.009 \\ 1.1592 \end{bmatrix} \frac{m}{s}$	$\begin{bmatrix} -4.6308 \\ -1.1194 \\ 4.2083 \end{bmatrix} \frac{m}{s}$	$\begin{bmatrix} -3.5876 \\ -1.7334 \\ 2.0011 \\ 4.6542 \end{bmatrix} \frac{m}{s}$	$\begin{bmatrix} -4.5921 \\ -1.7645 \\ -0.35844 \\ 1.8682 \\ 4.1578 \end{bmatrix} \frac{m}{s}$

4.2.2 *Maximization of Position Standard Deviation*

This case study introduces the proposed bi-level framework in the context of finding the maximal position standard deviation of the trajectory. Here, the standard deviations at each point of the trajectory are summed up and therefor an overall maximized results is sought rather than a result that exceeds the standard deviation of the reference case in each point. Again a minimization to the reference mean value from gPC is looked for to make the results comparable.

Now, Figure 3 introduces the mean trajectories to escape from the funnel. In the following figures, the reference results from standard gPC are depicted by a solid, red line, while the results of the proposed bi-level framework (worst-case) is given by a dashed, green line. It can be seen that the trajectories lie one above the other. This shows that the minimization to the reference mean value is successful and that the standard deviation results can be compared.

As it was already observed in subsection 4.2.1 the 3^{rd} and 5^{th} order expansion gave the best worst-case approximations of the response surface in this optimization setup. Therefor Figure 4 and Figure 5 give the corresponding standard deviation results for the 3^{rd} and 5^{th} of this case study respectively. A very similar behavior can be observed in the x-axis: The standard deviation increases with roughly a quadratic behavior. Also the results for the y-axis are very similar. Here, it can be seen that the standard de-

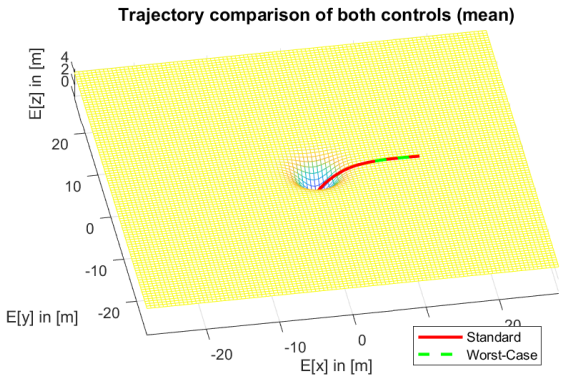

Fig. 3 : Mean optimized trajectory for reference (standard) gPC optimization and bi-level optimization (worst-case).

viation of the worst-case is reduced compared to the reference results. This shows the previously mentioned capability of the cost function to find a globally optimal solution instead of a solution that is worse in each point but might not be globally optimal. For the z-axis a rather different behavior can be seen: The 3^{rd} order expansion (Figure 4) is smaller overall but tends to a constant value in the end, while the 5^{th} order expansion (Figure 5) is larger overall but has a very similar behavior as the reference case.

This different behavior can also be seen looking at the cost function of the bi-level OC, i.e., in this case the upper level. The cost functions are given as follows:

$$\begin{aligned} |J_{UL}^{3rd}| &= 22.4035 \\ |J_{UL}^{5th}| &= 34.9636 \end{aligned} \tag{13}$$

Thus, Eq. 13 shows that the 5^{th} order expansion creates a more optimal result in the sense of the cost function for this case as it creates a larger cost index for the upper level (a maximization is the goal).

Concluding, the proposed bi-level methodology has again shown its applicability in the context of aircraft trajectory optimization to calculate worst-case trajectories. These results can be used to get an impression of the uncertainty interval and how the approximation might be in a worst-

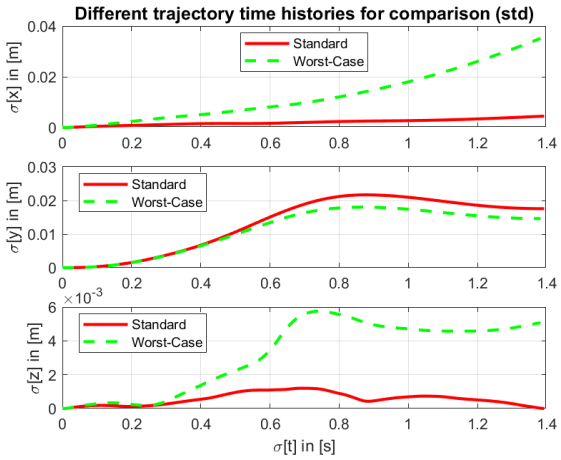

Fig. 4 : Comparison of standard deviation results for standard gPC and worst-case approximation with an order 3 expansion.

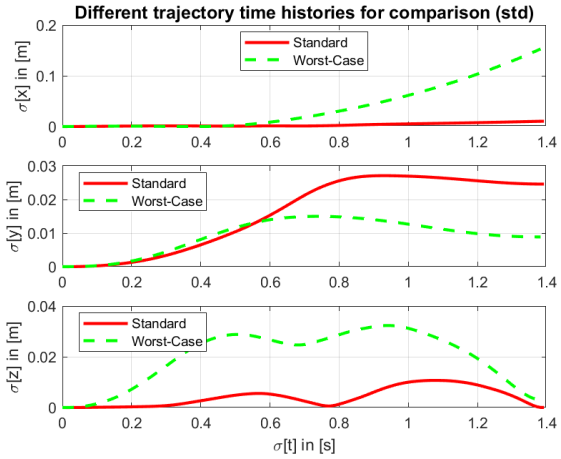

Fig. 5 : Comparison of standard deviation results for standard gPC and worst-case approximation with an order 3 expansion.

case sense.

5 Conclusion and Perspective

Within this study, we developed a methodology to calculate optimal trajectories with uncertainties and their worst-case approximations. For this, the gPC methodology is incorporated into a bi-level OC framework. A basic problem of the gPC method, namely the fact that the quality of the results for e.g., mean and standard deviation, have no defined bounds, is overcome using the bi-level formulation as it gives the possibility to calculate the worst-case bounds.
Here, the LAGRANGE collocation approach is used that makes it also possible to use the gPC methodology for uncertainty distributions not covered by the WIENER-ASKEY SCHEME. Within the bi-level approach the SC nodes are chosen in the upper level by a parameter optimization problem in a manner that the worst-case approximation for the lower level is achieved. The lower levels calculate the optimal trajectories at these SC nodes.
Future research should be concerned with a faster update of the upper level problem using sensitivities. Ultimately, the proposed framework is also not only limited to OC: On the contrary, the lower level provides also space for a simulative assessment. This could e.g., be used in the context of step responses to test a control circuit. Here, also worst-case LAGRANGE points are of interest to calculate a stability area of the control circuit.

6 Contact Author Email Address

patrick.piprek@tum.de

Acknowledgment

This research was supported by the Deutsche Forschungsgemeinschaft (DFG) through the TUM International Graduate School of Science and Engineering (IGSSE).
The authors wish to thank Florian Wachter who contributed the visualization and Michael Krenmayr who contributed the initial simulation model. Additionally, the authors wish to thank Johannes Diepolder and Benedikt Grueter for the discussions on optimal control related topics.

Copyright Statement

References

[1] D. Xiu and G. E. Karniadakis, "The wiener-askey polynomial chaos for stochastic differential equations," *SIAM Journal on Scientific Computing*, vol. 24, no. 2, pp. 619–644, 2002.

[2] M. V. C. de Souza, M. J. Colaço, and A. J. K. Leiroz, "Application of the generalized polynomial chaos expansion to the simulation of an internal combustion engine with uncertainties," *Fuel*, vol. 134, pp. 358–367, 2014.

[3] D. Xiu and G. E. Karniadakis, "Modeling uncertainty in flow simulations via generalized polynomial chaos," *Journal of Computational Physics*, vol. 187, no. 1, pp. 137–167, 2003.

[4] V. Vittaldev, R. P. Russell, and R. Linares, "Spacecraft uncertainty propagation using gaussian mixture models and polynomial chaos expansions," *Journal of Guidance, Control, and Dynamics*, vol. 39, no. 12, pp. 2615–2626, 2016.

[5] D. Xiu, "Fast numerical methods for stochastic computations - a review," *Communications in Computational Physics*, vol. 5, no. 2-4, pp. 242–272, 2009.

[6] M. R. Rufuie, E. Gad, M. Nakhla, and R. Achar, "Generalized hermite polynomial chaos for variability analysis of macromodels embeddedin nonlinear circuits," *IEEE Transactions*

on Components, Packaging and Manufacturing Technology, vol. 4, no. 4, pp. 673–684, 2014.

[7] G. Zhang, J. Bai, L. Wang, and X. Peng, "Uncertainty analysis of arbitrary probability distribution based on stieltjes process," in *2017 IEEE 21st Workshop on Signal and Power Integrity (SPI)*. Piscataway, NJ: IEEE, 2017, pp. 1–3.

[8] K. SEPAHVAND, S. MARBURG, and H.-J. HARDTKE, "Uncertainty quantification in stochastic systems using polynomial chaos expansion," *International Journal of Applied Mechanics*, vol. 02, no. 02, pp. 305–353, 2010.

[9] F. Augustin, A. Gilg, M. Paffrath, P. Rentrop, M. Villegas, and U. Wever, "An accuracy comparison of polynomial chaos type methods for the propagation of uncertainties," *Journal of Mathematics in Industry*, vol. 3, no. 1, p. 2, 2013.

[10] N. Wiener, "The homogeneous chaos," *American Journal of Mathematics*, vol. 60, no. 4, p. 897, 1938.

[11] T. Arens, F. Hettlich, Karpfinger Christian, U. Kockelkorn, K. Lichtenegger, and H. Stachel, Eds., *Mathematik*. Heidelberg: Spektrum, Akad. Verl., 2010.

[12] J. T. Betts, *Practical methods for optimal control and estimation using nonlinear programming*, 2nd ed., ser. Advances in design and control. Philadelphia, Pa: Society for Industrial and Applied Mathematics (SIAM 3600 Market Street Floor 6 Philadelphia PA 19104), 2010.

[13] M. Rieck, M. Bittner, B. Grüter, and J. Diepolder, "Falcon.m user guide," 2016. [Online]. Available: www.falcon-m.com

[14] A. Wächter and L. T. Biegler, "On the implementation of an interior-point filter line-search algorithm for large-scale nonlinear programming," *Mathematical Programming*, vol. 106, no. 1, pp. 25–57, 2006.

[15] V. Feoktistov, *Differential Evolution: In Search of Solutions*. New York: Springer, 2006.

[16] B. L. Stevens and F. L. Lewis, *Aircraft control and simulation*, 2nd ed. Hoboken, NJ: Wiley, 2003. [Online]. Available: http://www.loc.gov/catdir/bios/wiley046/2003043250.html